This is a self-archived preprint copy of the following article: G. G. Justice and P. K. Bowen, "Construction and Validation of a Slip Ring Test Bench Using 50 Years of Data," *2025 IEEE 70th Holm Conference on Electrical Contacts (HLM)*, San Antonio, TX, USA, 2025, pp. 1-8, doi: 10.1109/HLM51652.2025.11278317.

Construction and Validation of a Slip Ring Test Bench Using 50 Years of Data

Grant G. Justice
Research & Development
Deringer-Ney Inc.
Bloomfield, CT, USA
gjustice@deringerney.com

Patrick K. Bowen
Research & Development
Deringer-Ney Inc.
Bloomfield, CT, USA
pbowen@deringerney.com

***Abstract*— Design and validation of a modernized slip ring test bench at Deringer-Ney Inc. was performed, enabling simultaneous measurement of electrical noise, contact resistance, wear rate, and friction under controlled conditions. Validation against 1970s archival data confirmed reliable replication of historical performance metrics using Neyoro G and Neyoro 28A alloy rings and Paliney 7 brushes, while extended testing successfully captured cyclical variations in electrical performance closely correlated with environmental humidity. Interrupted rotation testing revealed significant stick-slip phenomena with load variations up to 20%, and optimization determined 100 kHz as the ideal sampling rate for characterizing electrical noise. The system establishes a foundation for comprehensive characterization of sliding electrical contacts while providing new insights into the complex interplay between mechanical wear, environmental factors, and electrical performance.**

Keywords*— *slip ring; test bench; noble metal; Paliney; Neyoro; electrical noise

I. Introduction

Sliding electrical contacts serve as critical components in numerous engineering applications requiring the transmission of electrical signals between moving and stationary elements. The basic objective of sliding contact systems is to transfer electrical information from a moving member to one that is stationary while maintaining signal fidelity. Ideally, this information would remain unchanged in any way, with the sliding junction behaving just as if it were a static joint. However, achieving this ideal condition presents significant challenges due to the inherent mechanical and electrical complexities at the sliding interface. Low energy sliding contacts—those operating in signal-level applications rather than power transmission—are particularly sensitive to small variations in contact resistance, impedance, and surface films [1]. These contacts must function reliably across diverse operating environments while minimizing electrical noise, wear, and frictional losses that could compromise signal integrity. As technologies advance toward higher data rates and miniaturization, understanding the fundamental behavior of sliding electrical contacts becomes increasingly important for ensuring reliable performance in critical applications ranging from intravascular ultrasound medical imaging to satellite potentiometric positioning systems.

The performance of sliding electrical contacts is governed by complex interactions at the micro-asperity level. As described by early researchers like Holm [2], electrical contact occurs at discrete micro-asperities where the two surfaces make metallic contact, creating constriction resistance that limits electron flow through the contact zone. This constriction resistance arises from the limited number of contact points comprising an effective area of contact that is much smaller than the overall metallic surface area. During sliding motion, variations in contact resistance occur over time and position due to several factors: surface film changes, physical parameters (*i.e.*, contact force and surface roughness), and contamination from wear debris and surface films leading to measurable noise in the signal transmission. For high frequency applications beyond DC, additional capacitive and inductive effects as well as non-linear resistance effects contribute. As noted by Dorsey *et al.* [3], electrical contacts contribute AC impedance in addition to DC resistance in high-frequency information transition applications, with factors like skin effects at high frequencies adding complexity to the circuit.

Broadly, the electrical noise in slip ring systems examined in the course of this study represents a complex interplay of several distinct phenomena. The sources of noise in this work can be loosely divided into sources of “gross noise,” “sliding noise,” “setup noise,” and “measurement noise.” Gross noise occurs when brushes momentarily lose physical contact with the ring surface due to kinetic variations like stick-slip motion or "ski jump" effects, as well as from large resistive surface artifacts that disrupt continuous contact. Sliding noise can be considered to emerge from the microscopic dynamics at the contact interface, specifically the puncturing of thin surface films and the formation of a-spots during sliding, thus creating instantaneous variations in conductivity. Setup noise stems from non-ideal physical configurations, such as ring runout or eccentricity, which produce cyclical variations in contact force and consequently fluctuating contact resistance. Finally, measurement noise encompasses the inherent limitations of the test apparatus itself, including electromagnetic interference, power supply fluctuations, and signal conditioning artifacts.

A. Noble Metal Alloys for Slip Rings

Noble metal alloys are known as the materials of choice for low energy sliding contacts due to their chemical nobility, electrical conductivity, and mechanical properties. Gold-based [4], [5], silver-based, and palladium-based [6] alloys, in particular, can be selected to provide an optimal combination of wear resistance and electrical conductivity. Noble metal alloys exhibit predictable and minimal oxidation rates, resulting in low and predicable contact resistances over extended operational lifetimes. Material selection directly impacts critical performance parameters: Neyoro™ gold-based alloys deliver exceptional noise characteristics and durability in precision applications, while Paliney® compositions offer superior mechanical stability under moderate contact forces and temperatures [7]. This intertwined relationship between material composition, structure, properties, and performance underscores why materials selection represents one of the most significant design considerations in sliding contact applications where signal integrity is paramount.

Environmental conditions significantly influence the electrical and mechanical performance of sliding contacts in low energy applications. Humidity plays a critical role, as adsorbed water plays a well-known role in boundary lubrication. Organic contaminants present in the environment can either catalyze beneficial or deleterious tribochemical reactions, as demonstrated with platinum group metal (PGM)-based sliding contacts which catalyze the creation of an undesirable tribopolymer that increases electrical noise [8]. Temperature fluctuations also attenuate the kinetics of surface chemical reactions, thereby altering the stability of the system over time. The interplay between these environmental factors and contact system necessitates careful material selection and environmental control strategies tailored to the specific operating conditions of the sliding contact system.

B. Prior Testing Approaches

A comprehensive test capability for slip ring sliding electrical contacts represents a critical asset for advancing both fundamental understanding and practical applications. By systematically evaluating the complex interactions between material wear mechanisms, environmental conditions, and electrical performance, causal relationships can be established that guide material selection and system design. The ability to conduct accelerated life testing under representative conditions was present at Deringer-Ney in the early 1960s, the mechanical portion of which is pictured in Figure 1. Further refinement enabling highly parallel testing was implemented in the 1970s. This experimental setup generated a wealth of data over the subsequent decade for applications research and publications, including the *Ney Scope* series and the *Ney Contact Manual* [1].

Tests conducted on these benches were characterized by electrically using tools available at the time. The 1970s incarnation was the best documented and was the focus of study and replication. The documented test conditions are summarized in Table 1.

Monitoring electrical noise in the 1970s work was performed on a circuit shown in Figure 2 by means of a HP 400E a-c millivoltmeter and Tektronix 502A oscilloscope. In this configuration, the perturbation voltage or current (depending on which was varied in each test) was subjected to conduction through three brushes, so the circuit comprised six brush-ring contact points. This arrangement is good for

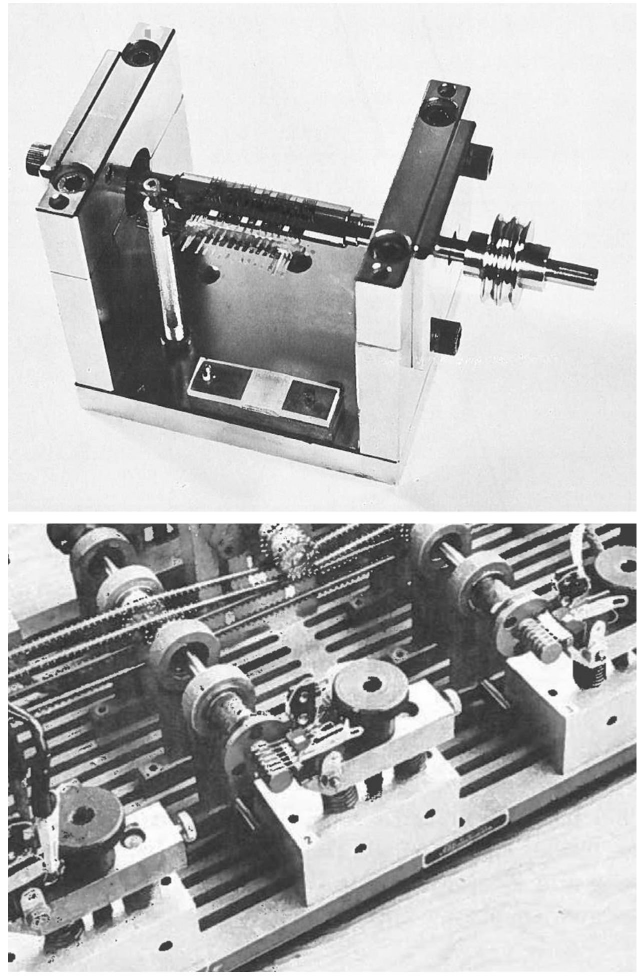

Figure 1 - 1960s-vintage slip ring tester used by the JM Ney Company [9] (top) and its 1970s-vintage counterpart designed for highly parallel slip ring testing [10] (bottom)

phenomenological study, as it tends to exaggerate the noise magnitude; noise source at any of the brush-ring contact points will cause an increase in the observed value. In most cylindrical slip ring applications, the two contact points per channel would function as a parallel circuit configuration.

Table 1 - Legacy slip ring test input variables used for comparison

Input Test Variable	Nominal	Range
Cleaning	Trichloroethylene degrease Ultrasonic clean Freon final clean	n/a
Voltage	11.0 V	†
Amperage	70. mA ‡	n/a
Rotation speed	1200 rpm, unidirectional	n/a
Relative humidity	Ambient, 30-60% RH	16-77% RH
Contact force	2 g_f	1.7-2.2 g_f
Lubrication	Boundary lubrication only	n/a
Test duration	n/a	630-1,110h

† Not disclosed ‡ Applicable to fixed-current test conditions only

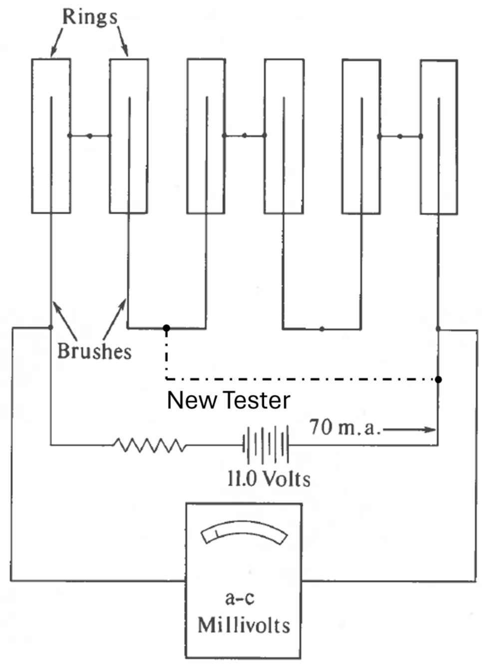

Figure 2 - Circuit used for 1970s (solid lines) and contemporary (broken line) measurements [10]

Furthermore, the 1970s work [10] concluded that:

- humidity had a negligible effect on wear rate;
- wear rates of the Neyoro G-Paliney 7 material couple exhibited wear of about 10^{-18} cm^2 g_f^{-1} on the brush and 10^{-14} cm^2 rev^{-1} g_f^{-1} on the ring;
- Neyoro G-Paliney 7 couple had a standard deviation of electrical noise 0.17-1.65 mV on an 11 V applied signal; and
- changing to a Neyoro 28A ring resulted in noise 500-1,000× higher.

A new slip ring test bench construction was sought at Deringer-Ney to continue research into basic materials interaction phenomena, environmental factors, and new applications as described prior. An opportunity arose to benchmark the new test system against its 50-year-old predecessor to qualify the design and operation of the new tester. Further data were also gleaned from the improved test system, including precise measurements of environmental conditions, brush displacement, and frictional forces.

II. Methods

A. Test Bench Construction

Test bench construction was carried out at Deringer-Ney Inc. after being adapted from a prototype design produced by the Blue Marble Security Student Enterprise at Michigan Technological University (Houghton, Michigan, USA). The assembly utilized a Maxon Motors (Sachseln, Switzerland) model 276508 400 W brushless motor coupled to the ring spindle with a belt drive. The motor included an optical encoder and was controlled by a Maxon Motors ESCON 70/10, 4-Q Servocontroller for DC/EC motors, with the control loop closed on velocity.

A signal was applied to the slip ring using a Fluke (Everett, Washington, USA) PM2811 600 W power supply in constant voltage mode. A 160 Ω resistor was placed in series with the slip ring limiting the current to the desired range. Voltage was supplied to a set of three brushes in parallel, passed though the rings, before returning though a second set of three brushes in parallel for an equivalent circuit shown in Figure 2. The voltage drop across the rings was measured using a Keithley (Cleveland, Ohio, USA) 7510 7.5-digit digital multimeter.

Three sections of ribbon were loaded into a brush block and wired in parallel. The brush block was adjustable such that all brushes contacted the ring at the same time. Load on each brush block was monitored using Transducer Techniques (Temecula, California, USA) RTS 0.04 N-m (5.5 in-oz) torque load cells. Unless otherwise specified, a flexible armature was secured between the torque load cell and the brush block to mitigate harmonic vibration. The tester was operated in a climate-controlled laboratory facility. A clear, flexible polyvinyl chloride (PVC) dust cover was secured over the tester.

Photographs of the slip ring tester's construction may be found in Figure 3.

Unless otherwise specified, data were collected for a "burst" period of 10 seconds at 100 Hz (number of power line cycles, NPLC = 0.44) data collection rate, with a frequency of once "burst" per minute. The resulting average voltage drop was converted to resistance and the standard deviation of resistance for each data set was reported.

B. Brush and Ring Materials

Solid precious metal brushes were fabricated internally at Deringer-Ney. Brushes were processed to 660 µm (0.026 inch) nominal diameter wire before being flat rolled to a thickness of 250 ± 10 µm (0.0100 ± 0.0004 in) thick by 1.02 ± 0.05 mm (0.040 ± 0.002 in) wide—a form selected for ease of fabrication in this study. Wrought hardenable alloys were left in the cold worked (CW) condition for testing. All other alloys were age hardened from the cold-worked (HTCW) condition prior to testing. Brushes were wiped with acetone using a clean lint free towel, then ultrasonically cleaned in isopropyl alcohol, and finally rinsed in flowing deionized water and dried with a lint-free towel prior to being installed on the slip ring tester.

Solid precious metal rings were also fabricated internally at Deringer-Ney by cold rolling and annealing plate castings starting at ~10 mm (~0.400 inches) thick. Age hardenable alloys were rolled to 2.5 mm (0.10 inches) thick and subsequently hardened from the cold worked condition. Wrought hardenable alloys were rolled to 1 mm (0.040 in) thick to achieve sufficient cold work to reach the targeted hardness. Rings were cut using wire electro discharge machining (EDM) into a washer shape with an outer diameter of 17.3 mm (0.680 in) and an inner diameter of 7.87 mm (0.310) inches—a form selected, again, for ease of fabrication. Washers were stacked and clamped in direct electrical contact on a low-runout collet.

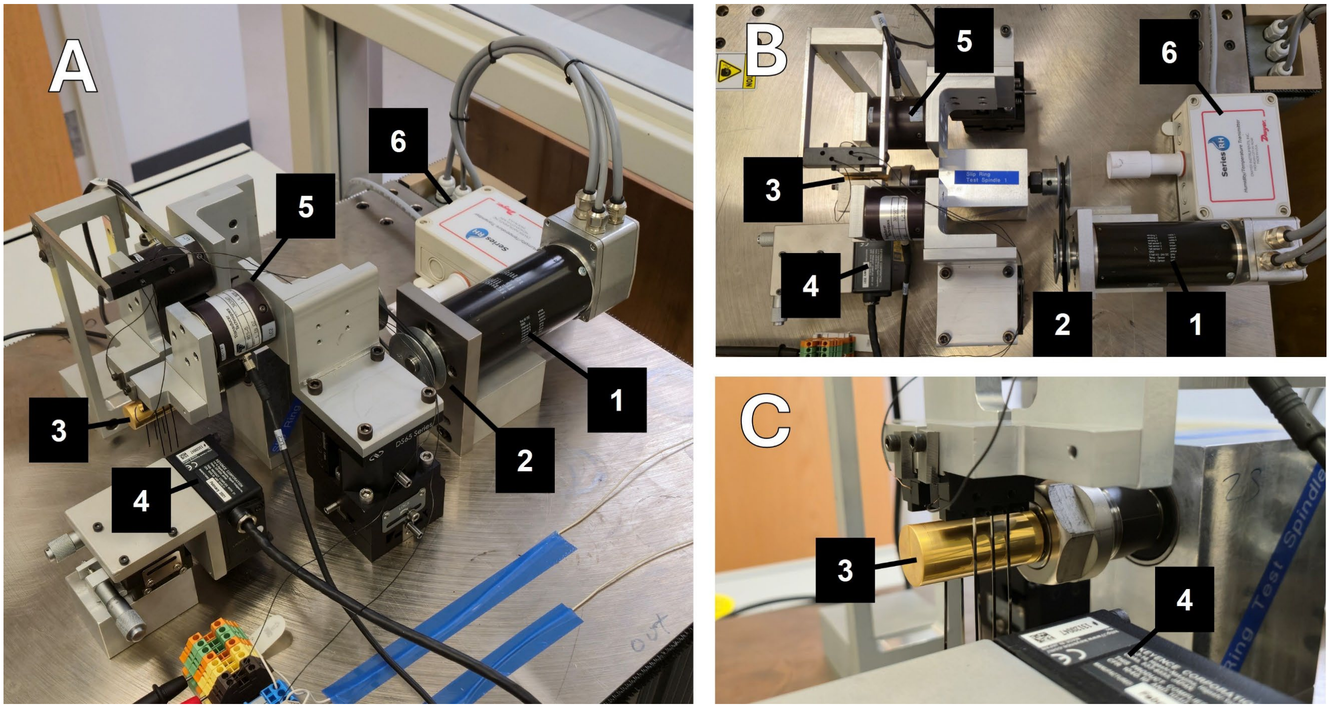

Figure 3 - Slip ring tester construction. Isometric (A), top-down (B), and detail (C) views illustrating the positions of the motor (1), belt drive (2), slip ring-brush assembly (3), laser displacement sensor (4), torque transducers (5), and temperature-humidity sensor (6). The detailed view (C) shows a close-up of the ring assembly—in this example a plated shaft rather than stacked washers—and three vertically oriented brushes.

Consequently, all rings were in physical and electrical contact on the shaft. The samples were ground on the test fixture to minimize runout before being polished using a sequence of 400-, 600-, 1,200-, 4,000-, 6,000-, and 8,000-grit polishing papers. After polishing, the rings were rinsed in flowing deionized water, then isopropyl alcohol, then again in deionized water. Hardness of the resultant materials were measured using a Leco (St. Joseph, Michigan, USA) M-400 hardness tester with a Knoop diamond indenter under 100 g_f load.

A summary of the material compositions and as tested hardnesses can be found in Table 2.

Table 2 – Nominal compositions and measured microhardness of tested materials

	Paliney 7	Neyoro G	Neyoro 28A
Ag (wt.%)	30	4.5	22
Au (wt.%)	10	71.5	75
Cu (wt.%)	14	14.5	-
Ni (wt.%)	-	-	3
Pd (wt.%)	35	-	-
Pt (wt.%)	10	8.5	-
Zn (wt.%)	1	1	-
Component	Brush	Ring	Ring
Material Temper	HTCW	HTCW	CW
Microhardness (HK_{100})	389	352	176

C. *Test and Interpretation*

Automation of the new slip ring test bench and data acquisition conforming to the aforementioned parameters was accomplished using National Instruments (Austin, Texas, USA) LabView software and a model 9201 data acquisition system. Measurements of electrical noise were analyzed as the population standard deviation, σ, of the voltage drop measured in each data collection "burst" over time. Unless stated otherwise, data visualizations omit 20-50% of data markers for readability.

III. Results & Discussion

Following prototype construction of the slip ring test bench at Michigan Technological University and subsequent refinement to improve assembly rigidity and data collection capabilities at Deringer-Ney, initial validation efforts focused on a well-characterized noble metal alloy wear couple of Paliney 7 brushes riding on Neyoro G rings. Initial efforts utilized an 8 VDC constant perturbation voltage, 50 mA nominal current, at 1,200 rpm rotation speed to replicate the 1970s operational parameters from Table 1. Using these parameters, a time *versus* voltage drop was collected and presented alongside 1970s data [10]. Figure 4 presents the juxtaposed data in a visually equivalent time domain; in general, the voltage drop magnitude that was observed correlated with the legacy data. Observed differences were generally related to data symmetry, which may be attributed to

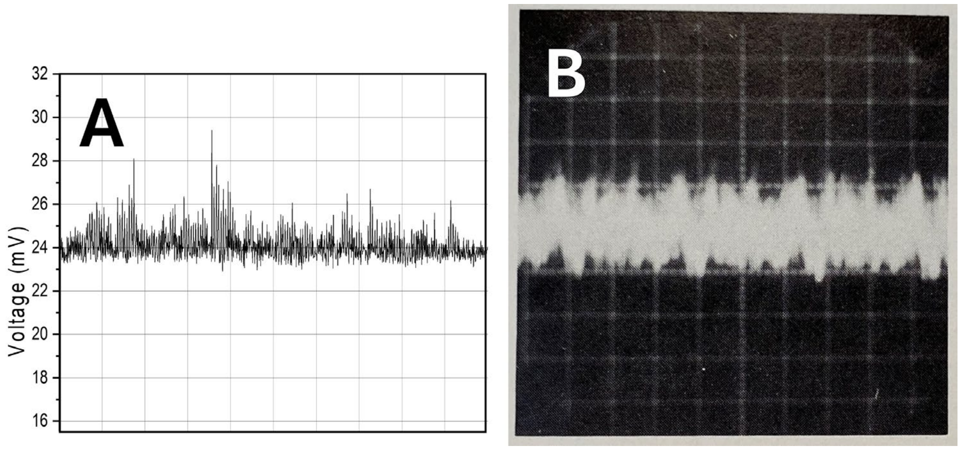

Figure 4 - Noise snapshot in the same voltage domain from the new test bench (A) and 1970s reference literature [10] (B) using a Paliney 7 brush on Neyoro G ring at 1,200 rpm. Data markers are omitted for readability.

technological differences in the acquisition methods, variability of the point in the testing at which the data were captured, and relative resolution of instruments separated in age by five decades. The lack of three rings in series would also be expected to reduce noise by 42% compared to the legacy data.

Next, the same test conditions were extended to a 24-hour acquisition period, and a comparison was prepared with the minima and maxima reported in the legacy data set. The results of this comparison are presented in Figure 5. 1970s data acquisition based upon periodic, manual readings and *ex post* statistical calculations did not allow for a direct time-based comparison. Nevertheless, comparisons of observed limits were compiled: the legacy observed minimum of 0.17 mV voltage drop variation compared well to the contemporary minimum noise value, and occasional voltage drop spikes to > 1 mV in the present measurements were similar to legacy observations of 1.17 mV on the high end. This was taken as a further positive correlation between old and new test methodologies and data interpretation.

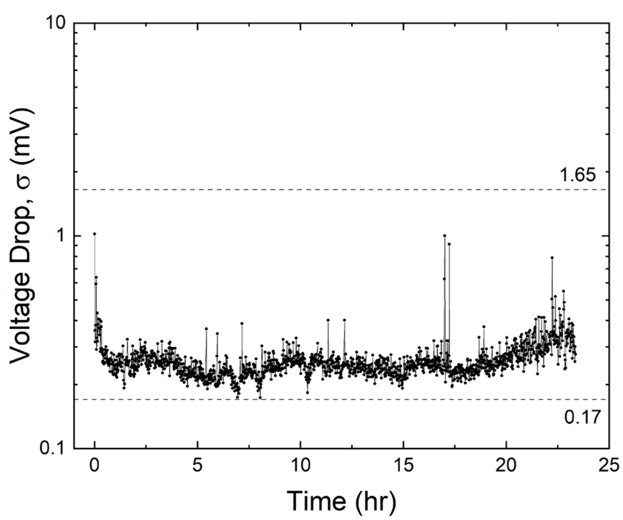

Figure 5 - Electrical noise test results from a one-day test of Paliney 7 on Neyoro G at 1,200 rpm, 11 VDC constant potential, and 70 mA nominal current juxtaposed with 1970s minimum and maximum voltage drop measurements (broken lines).

Following these cursory comparisons, a full set of data was collected from the same starting material couple covers a seven-day period of constant operation at 1,200 rpm. The resulting outputs of the modernized test apparatus are presented over identical time domains in Figure 6. Except for a single excursion at about 20 h, the rotational speed was well-controlled within 1% of 1,200 rpm by the Maxon motor-controller pair. Prior to about 54-60 h of operation, the output values of electrical noise, brush displacement, and the load on both brush blocks exhibited stable behavior, consistent with a "run-in" period of operation. Between about 60-66 h of operation, a transient was observed. In this narrow period, the voltage drop was observed to spike to a local maximum, brush deflection was observed to reach a minimum, and the load on both brush blocks was observed to move towards relative extremes. Taken holistically, this transient indicated a temporary increase in the sliding coefficient of friction, which may be associated with "breaking-in" of the wear couple and a corresponding, albeit brief, increase in adhesive wear characteristic of the Paliney 7-Neyoro G couple.

After the supposed "break-in" period, the slip ring system transitioned to predictable wear characterized by periodic undulations in noise, brush displacement, and both brush block load measurements. Each cycle is characterized by a rapid increase in system torque, a reduction in variation of the brush position, and a concomitant decrease in electrical noise (voltage drop). After the brush load reaches a maximum value, it gradually decreases over several hours until it plateaus at a value ~1-2 g_f less than the peak load. The load plateau region of each cycle corresponds to a higher observed variation in the brush position in addition to a higher degree of observed electrical noise. The wavelength of the cycles observed in the post-72 h period in Figure 6 is about 24 h. Periodicity in the electromechanical outputs of the test aligns well with observed environmental cycles. Daily minima in temperature resulting from laboratory facility temperature cycling were about 17-18°C (~63-65°F), while maxima were close to 23°C (74°F). During the 72-120 h period, two temperature cycles were observed with approximately constant relative humidity; the real moisture content of the laboratory atmosphere was highest at the maximum temperature. The increase in measured load on both brush blocks may be indicative of the peak of an adhesive transfer buildup on the brushes resulting in increased

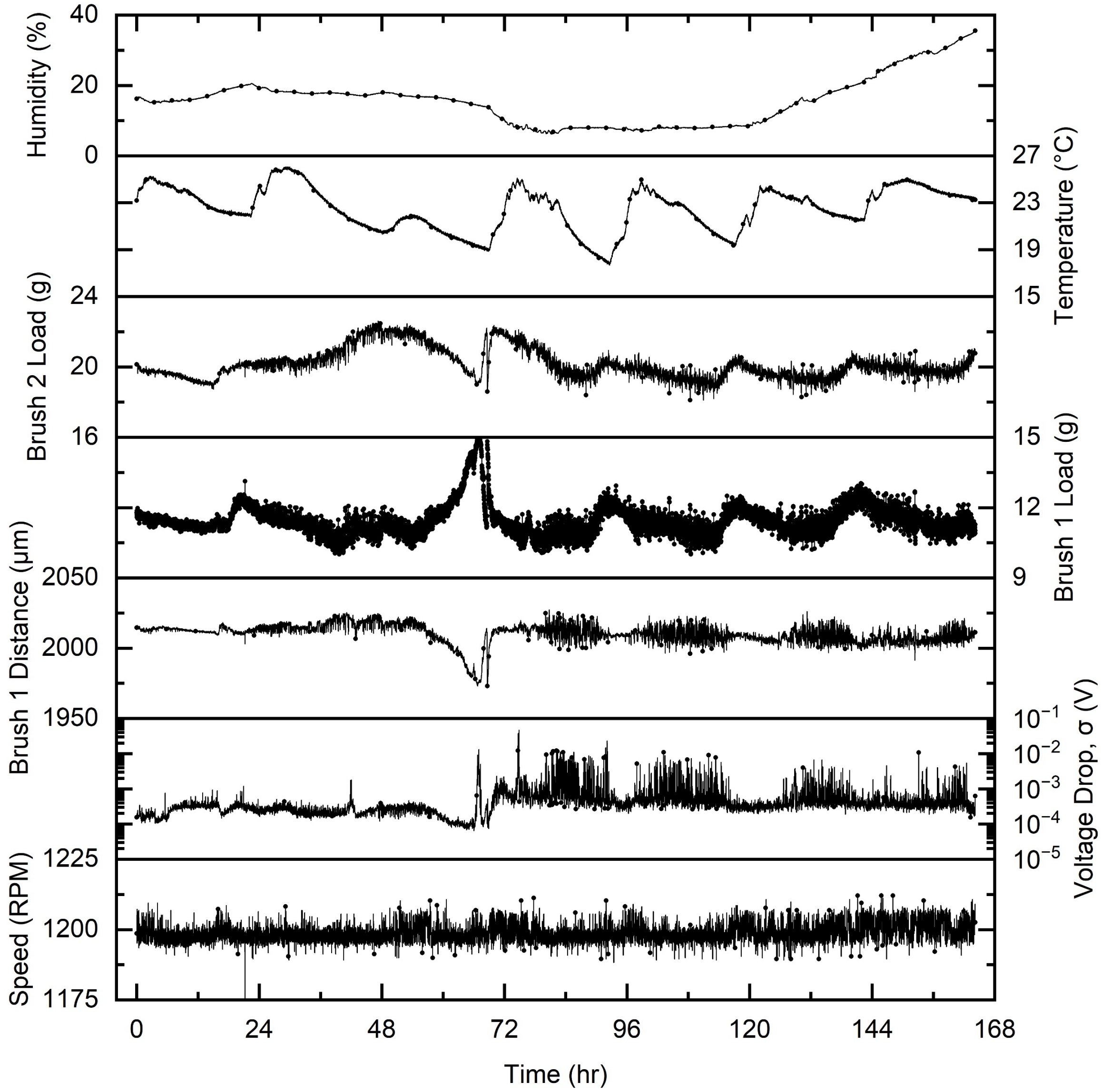

Figure 6 - Complete test data of Paliney 7 brushes on Neyoro G rings at 1,200 rpm, 70 mA nominal current, and 11 VDC constant potential over a seven-day period.

brush displacement and elastic loading. The frictional changes as absolute moisture content of the air drops with temperature may initiate a reversal of the adhesive transfer phenomena resulting in back-transfer of material to the ring reducing the height of the buildup with a commitment reduction in elastic loading of the brushes detected by the load cells. The period while the buildup back-transfers to the ring offered a more stable sliding regime with less stick-slip behavior evidenced by the reduction in noise on the load cell and laser displacement readings during this timeframe and contributing to the observed decrease in electrical noise. In general, the effects of humidity on sliding contact in model tribological systems [11] and simulated slip ring systems [12] and related shifts in wear mode are well-known. However, the associated load and position changes readily observable in this fully featured test system adds value to the engineering interpretation of the dataset.

Following this detailed study of a single system under fixed test conditions, a brief study of frictional force as a function of rotational conditions (first under constant speed and then under interrupted conditions) was conducted. The test velocity inputs and measured load outputs are compiled and presented in Figure 7. As observed in this figure, a 100-fold increase in monotonic rotation speed correlated to a very slight shift in the associated brush block load, about 1%. In contrast, the subsequent low speed, interrupted rotational regime produced periodic variations in brush load of around ± 8% in addition to isolated load excursions of up to about 20% in magnitude. The former was suspected to be related to a small but unavoidable runout in the test (brush position data omitted for brevity). The

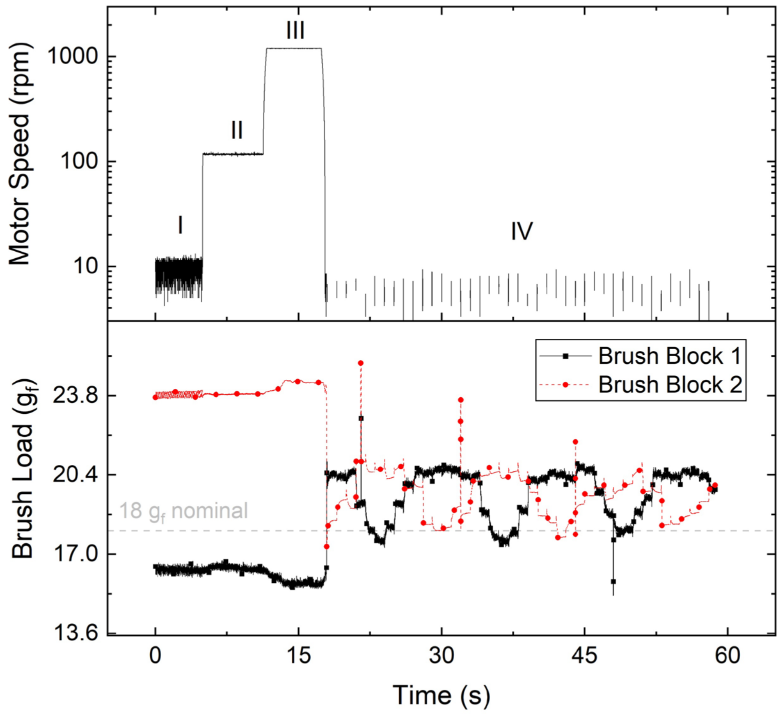

Figure 7 – Paliney 7 brushes on Neyoro G rings under a progression of increasing rotational speed of 10 (Region I), 120 (II), and 1,200 rpm (III) followed by interrupted rotation of 6 rpm for 1 second (IV) (top) and the associated brush load measurements for both blocks (bottom). The nominal brush block load of 18 g_f is indicated by a broken gray line. Markers omitted from the top plot for readability.

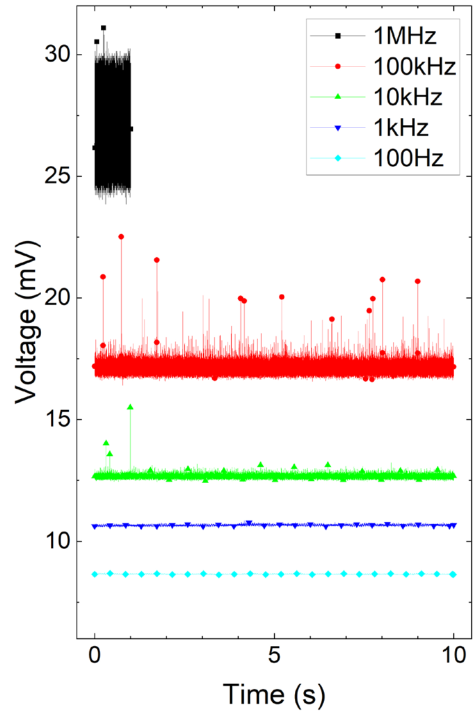

Figure 8 – Data collection rate effect of Paliney 7 brushes on Neyoro 28A rings under a nominal load of 6 g_f per brush (18 g_f per brush block), 1,200 rpm, 5 VDC fixed potential producing ~ 250 mA current. Results are offset in arbitrary y-axis increments for readability.

latter behavior is indicative of a stick-slip phenomenon, in which a-spots can become cold-welded and momentarily increase the coefficient of static friction when rotation resumes. Direct observation of this phenomenon is of use to the slip ring designer, who must ensure that the torque provided by any drive system(s) can overcome such events after a system has ceased rotation momentarily. Furthermore, the observation of at least four of these excursions within 40 seconds of operation suggests that the modern test bench design may be used to elucidate the statistical nature of stick-slip behavior on startup.

A final validation study of slip ring behavior using a different, higher-electrical noise system of Paliney 7 brushes on Neyoro 28A rings was conducted to evaluate the impact of data recording speed on the assessed voltage drop. The modern electronics were capable of logging rates of 100 Hz (the nominal rate used in the prior studies) to 1 MHz. Decadal increases in logging rate were tested on the same physical brush-ring pair and are presented on the same real time scale in Figure 8. Readily evident was a trend of increasing volatility in the acquired voltage drop data with increasing logging rate. The lowest data acquisition frequencies—100 Hz and 1kHz—exhibited no excursions to high voltage drop; this was unexpected and questionable, as the 1970s legacy data suggests that noise as significant as millivolts or tens of millivolts should be observable for this slip ring material couple. Increasing the data acquisition rate further to 10 kHz and 100 kHz increased the magnitude of basal noise and the magnitude and frequency of voltage drop excursions. Increasing the data acquisition rate further to 1 MHz has the effect of obscuring most system behavior (*i.e.*, “gross noise” and “sliding noise”) in electronic noise, potentially due to high-frequency capacitive effects [3], and rapidly filling the electronic instrument buffer thus limiting the total time period of data to one second. The *prima facie* result of this assessment is that the 100 kHz acquisition rate qualitatively matches the legacy description of electrical noise performance the Paliney 7 brush-Neyoro 28A ring pair.

Using the hardware and approaches described above, these individual contributions to electrical noise in a slip ring system and their respective causes may be analyzed. In the next phases of this research, deeper understanding of noise and wear may be achieved by the addition of volumetric wear assessments, topographical analysis of the wear scar and adjacent areas, evaluation of wear particulate geometries, and microchemical analyses of the wear scar, amongst other direct evaluations of this type. Understanding the unique contributions of each noise component and their respective underpinnings is critical for both accurate characterization of slip ring performance, accurately projecting the performance of a material couple in service, and for implementing effective design strategies to minimize noise in practical applications.

IV. Conclusions

This study successfully validated a newly constructed slip ring test bench against historical 1970s data, demonstrating excellent correlation when testing noble metal alloy rings and brushes. The modernized system provides unprecedented data fidelity through simultaneous high-resolution measurements of electrical noise, brush displacement, contact force, and environmental parameters. Environmental factors, particularly humidity cycling, were shown to significantly influence sliding contact behavior, with demonstrable correlations between temperature-humidity cycles and periodic variations in electrical and mechanical performance. Distinct operational phases were characterized, including initial run-in periods, transient break-in events, and established cyclical wear patterns. Testing of interrupted rotation revealed significant stick-slip phenomena with load variations up to 20% that would be critical factors in intermittent applications. Finally, data acquisition rate was found to be crucial in characterizing electrical noise, with 100 kHz emerging as optimal for capturing relevant characteristics without electronic artifacts on the new measurement apparatus. These improvements establish a foundation for systematic characterization of slip ring materials. Future work testing new noble metal alloy brush-ring pairs that were introduced in the previous few decades. A comparison of basic electrical contact phenomena in model systems (*i.e.*, using tribometry) as compared to a fully equipped slip ring tester could also be considered in future work.

Acknowledgment

The authors gratefully acknowledge Charles Psholka, Miguel Goncalves, and Ege Kayaarasi of Deringer-Ney Automation for their assistance in refining the test bench design and construction. Acknowledgement for test execution to Scott Marquis and Joe Cheney of Deringer-Ney Research & Development. Assistance for turning rings on centers was provided by Tom Hurst and Joseph Hurst of the Deringer-Ney Tool Room. Prototyping acknowledgement is owed to Michigan Technological University students Brent Bulgarelli, Emma Eke, Leighton Gaines, Sam Johnson, Phillips Munter, Alex Newman, Zarek Pirkola, Paola Quintana, John Ruf, and their faculty advisor, Prof. Glen Archer.

References

[1] K. E. Pitney, *Ney Contact Manual: Electrical Contacts for Low Energy Uses*, Revised 1st Edition. Bloomfield, Connecticut: Deringer-Ney Inc., 2022.

[2] R. Holm and E. Holm, *Electric Contacts: Theory and Application*. Springer, 1967.

[3] G. F. Dorsey, D. S. Coleman, and B. K. Witherspoon, “High speed data across sliding electrical contacts,” in *2012 IEEE 58th Holm Conference on Electrical Contacts (Holm)*, IEEE, 2012, pp. 1–12.

[4] A. A. Conte Jr and V. S. Agarwala, “An investigation of gold alloy slip ring capsule wear failures,” *Wear*, vol. 133, no. 2, pp. 355–371, 1989.

[5] R. Hayes, E. Mumm, and K. Gotthelf, “Electrical noise performance of gold-on-gold slip rings,” in *43th Aerospace Mechanisms Symposium, Santa Clara, California, USA*, 2016, pp. 345–357.

[6] M. Antler, “The development and application of palladium contact materials,” *Platinum Metals Review*, vol. 31, no. 1, pp. 13–19, 1987.

[7] T. V. Nordstrom, “Comparison of mechanical properties for several electrical spring contact alloys.,” Sandia National Laboratory; Albuquerque, New Mexico, USA, SAND-75-0365, Jun. 1976.

[8] W. Crossland and P. Murphy, “The formation of insulating organic films on palladium-silver contact alloys,” *IEEE Transactions on Parts, Hybrids, and Packaging*, vol. 10, no. 1, pp. 64–73, 1974.

[9] I. R. Bogue, “Frictional Wear of Metallic Contacts,” presented at the The Pennsylvania State University Electrical Contacts Seminar, University Park, PA, Jun. 1960.

[10] “Type 1420 Turrent Slip Ring - Type 1356 Brush Performance at 1200 RPM (Neyoro G Rings - Paliney 7 Brushes),” JM Ney Company, Bloomfield, Connecticut, S-69, 1973.

[11] Z. Chen, X. He, C. Xiao, and S. H. Kim, “Effect of Humidity on Friction and Wear—A Critical Review,” *Lubricants*, vol. 6, no. 3, Art. no. 3, Sep. 2018, doi: 10.3390/lubricants6030074.

[12] N. Argibay, J. A. Bares, and W. G. Sawyer, “Asymmetric wear behavior of self-mated copper fiber brush and slip-ring sliding electrical contacts in a humid carbon dioxide environment,” *Wear*, vol. 268, no. 3–4, pp. 455–463, Feb. 2010, doi: 10.1016/j.wear.2009.08.036.